Journal Name

COMMUNICATION

Acetylcholine-responsive cargo release using acetylcholinesterase-capped nanomaterials

Received 00th January 20xx,
Accepted 00th January 20xx

DOI: 10.1039/x0xx00000x

www.rsc.org/

Tania M. Godoy-Reyes,[abc] Antoni Llopis-Lorente,[abd] Alba García-Fernández,[abd] Pablo Gaviña,[abc] Ana M. Costero,[abc]* Ramón Martínez- Máñez,[abd]* and Félix Sancenón[abd]

Mesoporous silica nanoparticles capped with acetylcholinesterase, through boronic ester linkages, selectively release an entrapped cargo in the presence of acetylcholine.

Acetylcholine (ACh) is one of the most important neurotransmitters in the central nervous system (CNS) and in the peripheral nervous system (PNS).[1] ACh is synthesized in neuron terminals by acetylation of choline with acetyl coenzyme A in a reaction catalysed by the enzyme choline acetyltransferase.[2] In the CNS, ACh is responsible for modulating the activity of the neurons which control motivation, excitement and attention.[3] It is a key neurotransmitter to maintain memory and promote learning, in addition to favour brain neuroplasticity.[4] On the other hand in the PNS, ACh is responsible for transmitting signals between motor nerves and muscles, contributing to the contraction of the cardiac, skeletal and smooth muscles.[5] Low levels of ACh are related to neurodegenerative pathologies such as Alzheimer,[6] and myasthenia gravis.[7] In contrast, high levels of ACh are responsible for movement disorders such as dystonia[8] and Parkinson's disease.[9] The high concentrations of ACh in the movement disorders are caused by an imbalance between cholinergic and dopaminergic activity, generating a dopamine depletion which blocks the autoinhibition of acetylcholine release through muscarinic autoreceptors, leading to excessive acetylcholine release to the synaptic cleft.[10]

From another point of view, the design of smart delivery systems able to release an entrapped cargo in response to a specific stimulus is receiving increasing attention in recent years.[11] For the development of these smart delivery systems inorganic scaffolds, liposomes, polymers and metallic nanoparticles are commonly used as nanocarriers.[12] Among them, mesoporous silica (MS) scaffolds offer appealing features such as high loading capacity, uniform pore distribution, biocompatibility, thermal stability, easy synthesis, tuneable size and easy functionalization.[13] Additionally, the external surface of the loaded MS scaffold can be functionalized with molecular or (supra)molecular architectures which change their shape and/or size upon application of external stimuli.[14] In the absence of stimuli pores are blocked preventing cargo release whereas in their presence a marked delivery is observed. Gated MS materials that respond to physical and (bio)chemical stimuli have been developed.[15] Notwithstanding, the design of gated materials that respond to small biomolecules remains more challenging and comparatively fewer examples have been reported.[16]

Given the relevance of ACh as a key neurotransmitter and our interest in the development of stimuli-responsive gated materials for biomedical applications, we present herein a simple strategy to design ACh-responsive delivery systems based on the use of the enzyme acetylcholinesterase. Acetylcholinesterase is a glycoprotein that catalyses the breakdown of acetylcholine at the synaptic cleft. In our approach, acetylcholinesterase plays the following roles: (i) acts as capping agent, anchored to the external surface of the support through the formation of hydrolysable phenylboronic esters; (ii) acts as recognition unit, capable of detecting Ach; (iii) acts as anticholinergic agent by breaking down ACh, and, finally, (iv) acts as mediator agent, that generates acid molecules which induce the uncapping of the support. As a support, we have used MS nanoparticles that are loaded with a fluorescent cargo ($[Ru(bpy)_3]Cl_2$) and functionalized with phenylboronic acid residues on the external surface. Oligosaccharide groups of the enzyme are linked to phenylboronic acid residues by the formation of boronic acid cyclic esters, a well-known strategy previously used for the immobilisation of glycoproteins on electrodes and surfaces.[17] Acetylcholinesterase induces the rupture of ACh into choline and acetic acid. The later induces the hydrolysis of acid-sensitive boronic esters and the uncapping of the pores, resulting in cargo release (Scheme 1).

To prepare the ACh-responsive nanodevice, MS nanoparticles were synthesised via a sol-gel template method (solid **S0**). **S0** was suspended in acetonitrile and treated with (3-glycidyloxypropyl)trimethoxysilane for 5.5 h. Then, 3-aminophenylboronic acid was anchored by nucleophilic attack

[a] Instituto Interuniversitario de Investigación de Reconocimiento Molecular y Desarrollo Tecnológico (IDM), Universitat Politécnica de Valencia, Universitat de València, Spain.
[b] CIBER de Bioingeniería, Biomateriales y Nanomedicina (CIBER-BBN), Spain.
[c] Departamento de Química Orgánica, Universitat de València, Doctor Moliner 50, Burjassot, 46100, València, Spain. E-mail: ana.costero@uv.es
[d] Departamento de Química, Universitat Politécnica de València, Camino de Vera s/n, 46022, Valencia, Spain. E-mail: rmaez@qim.upv.es
Electronic Supplementary Information (ESI) available: Experimental details and further materials characterization. See DOI: 10.1039/x0xx00000x

of the amine to the highly reactive epoxide on the silica surface. The pores were loaded with the fluorescent dye $[Ru(bpy)_3]Cl_2$ as a model cargo (**S1**). **S1** was finally capped with acetylcholinesterase, via the formation of cyclic phenylboronic acid esters between the oligosaccharide chains of the glycoenzyme and the phenylboronic groups on the nanoparticles surface, yielding **S2**.

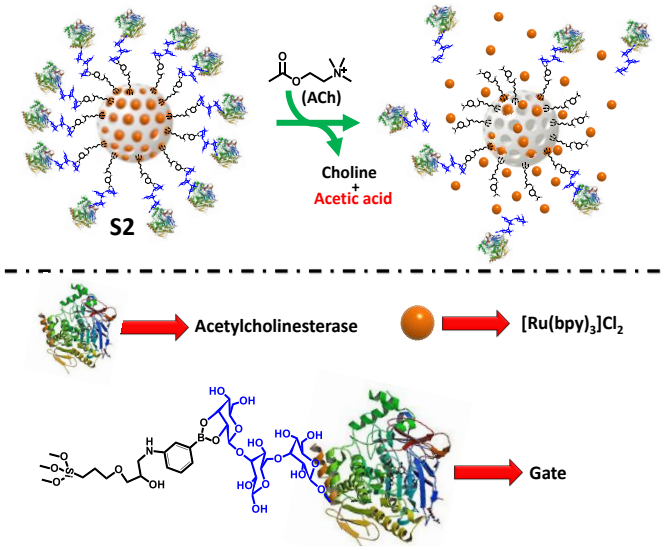

Scheme 1. Representation of the design and performance of the acetylcholinesterase-capped nanodevice **S2** for cargo release in response to ACh.

The prepared materials were characterised by different standard techniques. Powder X-ray diffraction (PXRD) of the as-made nanoparticles showed the (100) low-angle reflection Bragg peak at around 2.2° which is characteristic of MCM-41-type porous materials, with a slight displacement to 2.4° after surfactant removal (Figure 1A). The presence of this peak in the PXRD pattern of **S1** confirmed that the functionalization and loading processes had not damaged the mesoporous 3-D structure. From N_2 adsorption-desorption isotherms (Figure 1B), pore volume and pore size **S0** were determined as 0.715 $cm^3\ g^{-1}$ and 2.52 nm, respectively, by applying the BJH model[18] on the absorption branch of the isotherm. The volume of N_2 adsorbed considerably decreased from the empty solid **S0** to the loaded nanoparticles **S1** due to the filling of the pores with the cargo. A large specific surface area of 1141.13 $m^2\ g^{-1}$ was determined for **S0** according to the BET model,[19] whereas it reduced to 20.46 $m^2\ g^{-1}$ for **S1**. Transmission electron microscopy (TEM) images of **S0**, **S1** and **S2** confirmed the formation of nanoparticles (average diameter of 92±10 nm) with spherical morphology and porous structure, that was preserved after the functionalization processes (Figure 1C). Additionally, the surface modification was confirmed by chemical methods such as solid-state ^{13}C-NMR, ^{11}B-NMR, FTIR, and UV-visible (see Figure SI-1-4). The zeta potential of the starting **S0** nanoparticles was -30.5 mV and decreased to -12.7 mV for **S1** due to its functionalization with phenylboronic acid residues. For the final nanodevice **S2**, the surface charge increased (-24.1 mV) compared to **S1** as a consequence of enzyme capping (Figure SI-5). The hydrodynamic diameter of the final nanodevice **S2** was determined to be 152 nm using dynamic light scattering (DLS) measurements (Figure SI-6). Besides, the content of grafted aminophenylboronic moiety (53 mg per g of solid) and $[Ru(bpy)_3]Cl_2$ (270 mg per g of solid) on **S1** were estimated by elemental analysis. The boron and ruthenium content were determined by ICP-mass spectroscopy and amounted to 5.10±0.03 and 44.7±0.3 mg per g of **S1**, respectively. Moreover, the immobilization of acetylcholinesterase on **S2** was confirmed by a specific enzymatic assay (Figure SI-7). Additionally, the amount of protein was quantified as 58.5 mg per g of **S2** according to the Bradford method. The key role played by the phenylboronic linker in the attachment of the enzyme was confirmed by control experiments using non-functionalized MS nanoparticles (see SI, Section 9). The total loaded $[Ru(bpy)_3]Cl_2$ dye in the final nanodevice **S2** was 34 mg g^{-1} (determined via several extractions of the dye content in water at pH 3, and spectrophotometric measurement). Finally, Figure 1D shows scanning transmission electron microscopy coupled with energy dispersive X-ray spectroscopy (STEM-EDX) mapping of several elements on the final nanodevice **S2** attributed to the different components: Si and O (silica scaffold), C and N (cargo, aminophenylboronic moiety and enzyme), B (boronic ester), and S (cysteine groups of the enzyme).

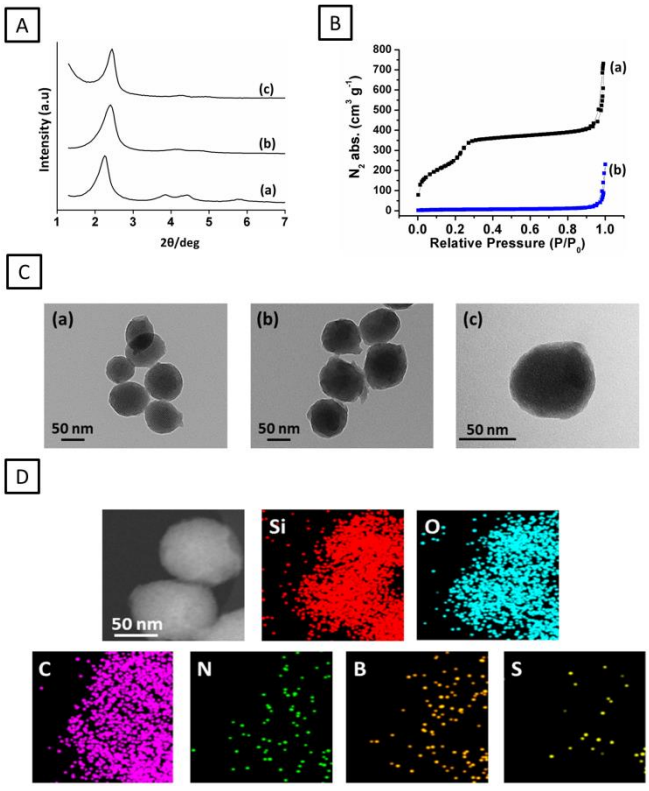

Figure 1. A) PXRD of (a) as-made MS nanoparticles, (b) calcined support **S0**, and (c) loaded and functionalized nanoparticles **S1**. B) N_2 adsorption-desorption isotherm for (a) **S0** and (b) **S1** nanoparticles. C) TEM images of (a) **S0**, (b) **S1**, and (c) final nanodevice **S2**. D) STEM image and STEM-EDX mapping of different atoms on the final nanodevice **S2**.

Once characterized, cargo release from **S2** was evaluated in aqueous media in the absence and presence of ACh. In a typical release experiment, aqueous (pH 7.5, 20 mM Na_2SO_4) **S2** suspensions (2 mg mL^{-1}) in the absence and in the presence of ACh (1 mM) were shaken at room temperature. Aliquots were taken at different times, centrifuged (to eliminate the nanoparticles), and the amount of cargo released to the solution was assessed by measuring the emission band of $[Ru(bpy)_3]Cl_2$ at 595 nm (λ_{exc}=435 nm). The obtained delivery kinetics profiles are shown in Figure 2. In the absence of ACh, cargo release from **S2** was negligible which confirms the correct

capping of the nanoparticles. On the contrary, in the presence of ACh, a remarkable and fast delivery of the payload was observed in less than 5 minutes, which could be appreciated even to the naked eye (Figure SI-11). This fast and effective response is attributed to the rapid action of acetylcholinesterase (turnover number=7.4 x 10^5 min^{-1})[20] which is an enzyme naturally prepared to catalyse very fast in order to regulate muscle contraction and synaptic transmission in the nervous system. ACh is hydrolysed by the enzyme into choline and acetic acid (pK_a=4.75),[21] which triggers the rupture of the acid-sensitive boronic cyclic esters and results in the detachment of the enzyme and the delivery of the payload. A reduction in the pH of the solution was observed after release experiment in the presence of ACh, thus confirming the formation of acetic acid (Figure SI-15). Furthermore, in order to confirm enzyme detachment from the nanoparticles surface, we measured the acetylcholinesterase activity on **S2** after ACh-triggered release and it decreased to 0.4 U mg^{-1} (4.5 U mg^{-1} for the control sample) (Figure SI-12). In further control experiments, we confirmed that the release from **S2** is triggered at acidic pH (4.5). However, **S2** remained capped at slightly acidic pH (6.5) such as the one found in tumours and some intracellular compartments (Figures SI-16-17).[22] On the other hand, release experiments with **S1** (without the enzyme) in the presence and absence of ACh were also carried out. The obtained results (Figure SI-18) showed a marked cargo release in both cases. This confirms the key role played by the enzyme on the performance of the nanodevice.

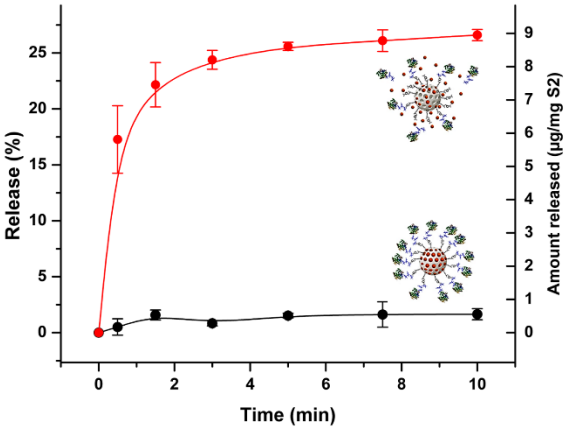

Figure 2. Kinetics of cargo release from **S2** (2 mg mL^{-1}) in aqueous media (pH 7.5) in the presence of ACh (1 mM, red curve) and absence of ACh (black curve) determined by measuring $[Ru(bpy)_3]Cl_2$ fluorescence at 595 nm (λ_{exc}= 453 nm). Error bars correspond to the s. d. from three independent experiments.

In order to assess the selectivity of the nanodevice, we evaluated the response of aqueous suspensions of **S2** (2 mg mL^{-1}) in the presence of other relevant neurotransmitters such as epinephrine (Epy), norepinephrine (NE), dopamine (DA), serotonin (5-HT), γ-aminobutyric acid (GABA), glutamate (Glu), asparate (Asp), and glycine (Gly) at 1 mM concentration. The obtained emission intensities at 595 nm (due to $[Ru(bpy)_3]Cl_2$ release) after 10 min are shown in Figure 3. As could be seen, **S2** nanodevice remained closed in the presence of these neurotransmitters whereas a selective cargo release occurred only in the presence of ACh, suggesting than **S2** could be used for the selective detection of ACh.

In order to evaluate the sensitivity of the nanodevice, **S2** nanoparticles were exposed to different concentrations of ACh and the released cargo at a fixed time (10 min) was measured. As can be observed in Figure SI-10, the amount of cargo release was very low at acetylcholine concentrations below 25 μM, whereas a significant and proportional increase occurred in the 0.025–10 mM concentration range. This indicates that **S2** would remain closed in blood, where the concentration of ACh is around 9 nM.[23] In contrast, in patients suffering from Parkinson's disease the levels of ACh in synaptic vesicles, neuromuscular junctions and synaptic clefts are higher than 100 mM, 3 mM and 0.5 mM respectively,[23] suggesting than **S2** nanoparticles could be able to release the cargo in these target regions.

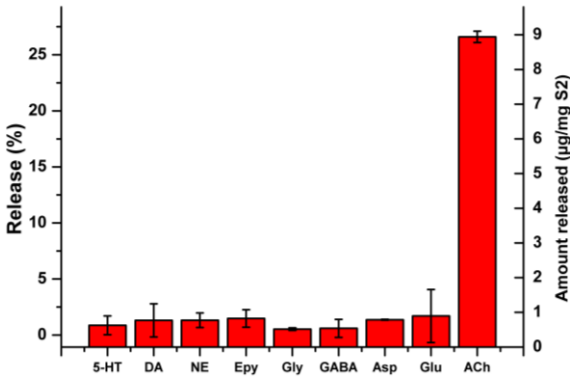

Figure 3. Cargo release from **S2** (2 mg mL^{-1}) in aqueous media (pH 7.5) in the presence of selected neurotransmitters (1 mM) after 10 min.

Finally, we aimed to demonstrate that this delivery system could operate in more complex biological environments. To this end, we prepared $\mathbf{S2_{dox}}$, a solid like **S2** but loaded with the cytotoxic drug doxorubicin. The amount of loaded doxorubicin was quantified as 195 mg per g of $\mathbf{S2_{dox}}$ by spectrophotometry, with a release efficiency of ca. 31% in *in vitro* release experiments conducted in a similar way as describe above (Figure SI-20). Next, as a proof of concept, human HeLa cell[24] culture media (DMEM supplemented with 10% FBS)[25] were treated with 50 μg mL^{-1} of $\mathbf{S2_{dox}}$ for 30 min, washed to remove non-internalized particles and further incubated for 24 h in the absence or presence of ACh (50 mM). After 24 h of incubation, cell viability was determined by means of the WST-1 cell proliferation reagent. Cell viability remained nearly to 100% in the presence of ACh or in the presence of $\mathbf{S2_{dox}}$, whereas it reduced to 72% upon treatment with the equivalent amount of free doxorubicin (Figure 4A). Remarkably, a significant reduction in cell viability (ca. 40%) was observed in the simultaneous presence of both, $\mathbf{S2_{dox}}$ and ACh, which was ascribed to the recognition of the neurotransmitter by the nanodevice and the subsequent release of the drug. Additionally, release of doxorubicin in cells was directly visualized by means of confocal microscopy imaging. For these experiments, cells were incubated with $\mathbf{S2_{dox}}$ for 2 h in the absence or presence of ACh, washed to remove non-internalized particles and stained with DNA marker Hoechst 3342 (blue). A clear doxorubicin-associated fluorescence (red) was observed for cells treated with $\mathbf{S2_{dox}}$ in a culture media containing ACh (Figure 4B). These results confirm the ability of the nanodevice to recognise ACh and deliver the payload despite the presence of cellular metabolites and other potential interferences found in cell culture media.

In conclusion, we report herein the design, synthesis and characterization of ACh-responsive delivery nanocarriers, based on the use of MS nanoparticles capped with the enzyme

acetylcholinesterase using boronic ester linkers. In the presence of ACh, the neurotransmitter is detected by acetylcholinesterase and transformed into choline and acetic acid, which leads to the hydrolysis of boronic cyclic esters, the subsequent detachment of the enzyme and the uncapping of pores. The nanoparticles show a remarkable payload delivery in the presence of ACh in less than 5 min, whereas release is negligible in the absence of the neurotransmitter. Moreover, the nanodevice remains closed in the presence of other relevant neurotransmitters and responds selectively to ACh. Cargo release is negligible at ACh concentrations present in human blood, whereas a significant payload delivery is observed in the 0.025-10 mM range, which coincides with typical concentration of ACh in synaptic vesicles, neuromuscular junctions and synaptic clefts in Parkinson's patients. We also demonstrate that the nanodevice shows an ACh-responsive behaviour in complex biological environments such as HeLa cells. We hope this study could inspire the development of smart nanosensors able to selectively detect ACh and/or nanocarriers for therapies with high effectiveness and minimal side effects for the future treatment of nervous system disorders such as Parkinson's.

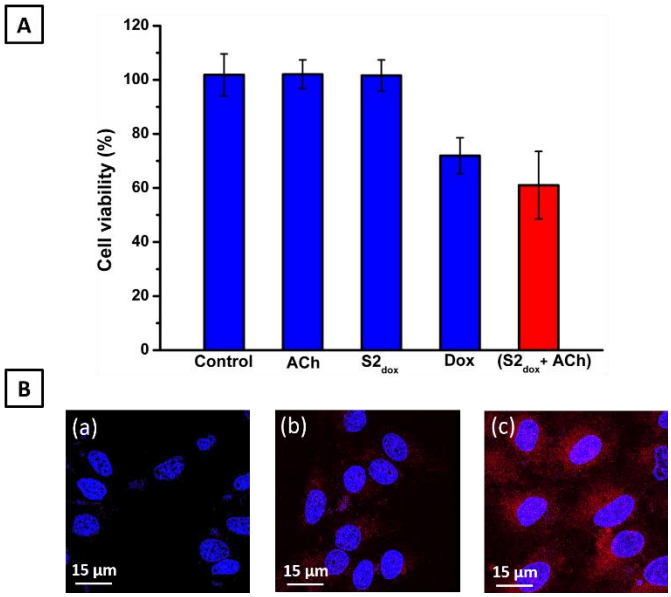

Figure 4. Experiments in cell culture media (DMEM supplemented with 10% FBS). A) HeLa cell viability for the control experiment (no ACh and no **S2**$_{dox}$), incubation with ACh (50 mM), incubation with **S2**$_{dox}$ (50 µg mL^{-1}), incubation with the equivalent amount of free doxorubicin, and incubation with both ACh and **S2**$_{dox}$. Error bars correspond to the s. d. from three independent experiments containing triplicates. B) Confocal microscopy images of HeLa cells (showing nuclei-marker fluorescence in blue) for: (a) control experiment, (b) cells incubated with **S2**$_{dox}$, and (c) cells incubated with **S2**$_{dox}$ in a medium containing ACh showing doxorubicin-associated fluorescence in red.

The authors acknowledge financial support from the Spanish Government (MAT2015-64139-C4-1-R and AGL2015-70235-C2-2-R) and the Generalitat Valenciana (PROMETEO2018/024). T. Godoy-Reyes is grateful to Generalitat Valenciana for her Santiago Grisolía fellowship. A. García-Fernández is grateful to the Spanish Government for her FPU fellowship.

References

1 L. K. McCorry, Am. *J. Pharm. Educ*., 2007, **71**, 78.
2 W. M. Haschek, C. G. Rousseaux and M. A. Wallig. Nervous System. In: Fundamentals of Toxicologic Pathology (Second edition). San Diego: Academic Press CY, 2010, 377.
3 I. Klinkenberg, A. Sambeth and A. Blokland, *Behav. Brain. Res*., 2011, **221**, 430.
4 (a) M. E. Hasselmo, *Curr. Opin. Neurobiol*., 2006, **16**, 710.
5 (a) M. C. An, W. Lin, J. Yang, B. Dominguez, D. Padgett, Y. Sugiura, P. Aryal, T. W. Gould, R. W. Oppenheim, M. E. Hester, B. K. Kaspar, C. P. Ko and K. F. Lee, *Proc. Natl. Acad. Sci. U. S. A*., 2010, **107**, 10702.
6 (a) G. Ehrenstein, Z. Galdzicki and G. D. Lange, *Biophys. J*, 1997, **73**, 1276.
7 (a) D. M. Fambrough, D. B. Drachman and S. Satyamurti, *Science*, 1973, **182**, 293; (b) D. B. Drachman, R. N. Adams, E. F. Stanley and A. L. A. N. Pestronk, *J. Neurol. Neurosurg. Psychiatry*, 1980, **43**, 601.
8 (a) D. E. Casey, J. Gerlach and E. Christensson, *Psychopharmacology*, 1980, **70**, 83; (b) J. Jankovic, *Lancet. Neurol*., 2006, **5**, 864.
9 A. L. Bartels and K. L. Leenders, *Cortex*, 2009, **45**, 915.
10 (a) T. Aosaki, M. Miura, T. Suzuki, K. Nishimura and M. Masuda, *Geriatr. Gerontol. Int*., 2010, **10**, S148; (b) P. Calabresi, B. Picconi, L. Parnetti and M. Di Filippo, *Lancet. Neurol*., 2006, **5**, 974; (c) S. Perez-Lloret and F. J. Barrantes, *NPJ Parkinsons Dis*., 2016, **2**, 16001; (d) O. B. Tysnes and A. Storstein, *J. Neural. Transm*., 2017, **124**, 901.
11 S. Mura, J. Nicolas and P. Couvreur, *Nat. Mat.*, 2013, **12**, 991.
12 (a) B. S. Pattni, V. V. Chupni and V. P. Torchilin, *Chem. Rev.*, 2015, **115**, 10938; (b) K. Ulbrich, K. Holá, V. Subr, A. Bakandritsos, J. Tucêk, and R. Zboril, *Chem. Rev.* 2016, **116**, 5338
13 (a) F. Tang, L. Li and D. Chen, *Adv. Mater.*, 2012, **24**, 1504; (b) Z. Li, J. C Barnes, A. Bosoy, J. F. Stoddart and J. I. Zink, *Chem. Soc. Rev*, 2012, **41**, 2590.
14 (a) J. Wen, K, Yang, F. Liu, H. Li, Y. Xu and S. Sun, *Chem. Rev.* 2017, **46**, 6024; (b) N. Song, and Y.-W. Yang, *Chem. Soc. Rev.* 2015, **44**, 3474.
15 E. Aznar, M. Oroval, L. Pascual, J. R. Munguia, R. Martínez-Máñez, and F. Sancenón, *Chem. Rev.* 2016, **116**, 561
16 F. Sancenón, L. Pascual, M. Oroval, E. Aznar and R. Martínez-Máñez, *ChemistryOpen*, 2015, **4**, 418.
17 (a) J. M. Abad, M. Vélez, C. Santamaría, J. M. Guisán, P. R. Matheus, L. Vázquez, I. Gazaryan, L. Gorton, T. Gibson and V. M. Fernández, *J. Am. Chem. Soc*., 2002, **124**, 12845; (b) Y. Zhao, B. G. Trewyn, I. I. Slowing and V. S.-Y. Lin, *J. Am. Chem. Soc*., 2009, **131**, 8398; (c) P. Díez, B. Esteban-Férnandez de Ávila, D. E. Ramírez-Herrera, R. Villalonga and J. Wang, *Nanoscale*, 2017, **9**, 14307.
18 E. P. Barrett, L. G. Joyner and P. P. Halenda, *J. Am. Chem. Soc*., 1951, **73**, 373.
19 S. Brunauer, P. H. Emmett and E. Teller, *J. Am. Chem. Soc*., 1938, **60**, 309.
20 I. B. Wilson and M. A. Harrison, *J. Biol. Chem.*, 1961, **236**, 2292.
21 N. V. Narendranath, K. C. Thomas and W. M. Ingledew, *J. Ind. Microbiol Biotechnol*., 2001, **26**, 171.
22 (a) N. Zhang, F. Zhao, Q. Zou, Y. Li, G. Ma and X. Yan, *Small*, 2016, **12**, 5936; (b) J. Kneipp, H. Kneipp, B. Wittig and K. Kneipp, *J. Phys. Chem. C*, 2010, **114**, 7421.
23 (a) C.-I. Wang, W.-T. Chen and H.-T. Chang, *Anal. Chem.*, 2012, **84**, 9706; (b) A. Schena and K. Johnsson, *Angew. Chem. Int*. Ed., 2014, **53**, 1302; (c) E. S. Vizi, A. Fekete, R. Karoly and A. Mike, *Br. J. Pharmacol.* 2010, **160**, 785; (d) Y. Zhou, L.-L. Tan, Q.-L. Li, X.-L. Qiu, A.-D. Qi, Y. Tao and Y.-W. Yang, *Chem. Eur. J.*, 2014, **20**, 2998.
24 (a) W. F. Scherer, J. T. Syverton and G. O. Gey, *J. Exp. Med.*, 1953, **97**, 695, (b) E. Boatman, F. Cartwright and G. Kenny, *Cell Tiss. Res.*, 1976, **70**, 1; (c) S. Prylutska, R. Bilyy, M. Overchuk, A. Bychko, K. Andreichenko, R. Stoika, W. Rybalchenko, Y. Prylutskyy, N. G. Tsierkezos and U. Ritter, *J. Biomed. Nanotechnol.*, 2012, **8**, 522; d) P. Díez, A. Sánchez, M. Gamella, P. Martínez-Ruíz, E. Aznar, C. de la Torre, J. R. Murguía, R. Martínez-Máñez, R. Villalonga and J. M. Pingarrón, *J. Am. Chem. Soc*., 2014, **136**, 9116.
25 S. Li, Q. Zou, Y. Li, C. Yuan, R. Xing and X. Yan, *J. Am. Chem. Soc.*, 2018, **140**, 10794.